

# Searching for magnetic fields in featureless white dwarfs with the DIPOL-UF polarimeter at the Nordic Optical Telescope

A. Berdyugin<sup>1</sup>, J. D. Landstreet<sup>2,3</sup>, S. Bagnulo<sup>2</sup>, V. Piirola<sup>1</sup>, and S. V. Berdyugina<sup>4,5,6</sup>

<sup>1</sup> Department of Physics and Astronomy, FI-20014 University of Turku, Finland  
e-mail: andber@utu.fi

<sup>2</sup> Armagh Observatory & Planetarium, College Hill, Armagh BT61 9DG, UK  
e-mail: Stefano.Bagnulo@Armagh.ac.uk

<sup>3</sup> University of Western Ontario, London, Ontario N6A 3K7, Canada  
e-mail: jlandstr@uwo.ca

<sup>4</sup> IRSOL Istituto Ricerche Solari "Aldo e Cele Daccò", Faculty of Informatics, Università della Svizzera italiana, Via Patocchi 57, Locarno, Switzerland

<sup>5</sup> Euler Institute, Faculty of Informatics, Università della Svizzera italiana, Via la Santa 1, 6962 Lugano, Switzerland

<sup>6</sup> Institut für Sonnenphysik (KIS), Georges-Köhler-Allee 401A, 79110 Freiburg, Germany

Received April 1, 2024; accepted

## ABSTRACT

About 20% of the white dwarfs possess a magnetic field that may be detected by the splitting and/or polarization of their spectral lines. As they cool, the effective temperatures of the white dwarfs becomes so low that no spectral lines can be seen in the visible wavelength range. If their atmospheres are not polluted by the debris of a planetary system, these cool white dwarfs have featureless optical spectra. Until quite recently, very little was known about the incidence of magnetic fields in these objects. However, when observed with polarimetric techniques, a significant number of featureless white dwarfs reveal strong magnetic fields in their optical continuum spectra. Measuring the occurrence rate and strength of magnetic fields in old white dwarfs may help us to understand how these fields are generated and evolve. We report the results of an ongoing survey of cool white dwarfs with the high-precision broad-band polarimeter DIPOL-UF, which is deployed at the Nordic Optical Telescope on La Palma, Spain. This survey has led to the firm discovery of 13 cool magnetic white dwarfs in the solar neighborhood so far, including six new detections that we report in this paper.

**Key words.** polarization – stars: white dwarfs – stars: magnetic fields

## 1. Introduction

White dwarfs (WDs) are the final evolution stage of at least 90% of all stars when the useable nuclear fuel is exhausted. These objects ( $M \sim 0.6M_{\odot}$ ,  $R \sim 0.01R_{\odot}$ ) are common in space around the Sun; about 150 of them are found within a distance of 20 pc (Hollands et al. 2018b). The basic evolution of a WD, which initially formed by the collapse of a stellar core, is to cool slowly on a timescale of several billion years. The physics of WDs has recently been reviewed by Saumon et al. (2022). However, this evolution is found to be surprisingly complex, for example because magnetic fields are present in more than 20% of the WDs (e.g., Bagnulo & Landstreet 2021).

Magnetic fields have been detected in several hundred nearby WDs, mostly through Zeeman splitting of spectral lines that were observed in flux spectra (e.g. Ferrario et al. 2020). The fields cover a wide range of strengths, from below  $10^4$  G up to nearly  $10^9$  G. In a volume-limited survey within 20 pc around the Sun, fields were detected in 20–25% of the WDs that were surveyed (Bagnulo & Landstreet 2021). The fields do not appear to evolve with time on an observable timescale, although they are often not symmetric about the rotation axis of the host WD and thus appear to vary periodically as the star rotates. A geometrical model for a star with a dipolar field that is tilted with respect to the rotation axis was developed for the magnetic Ap and

Bp stars by Stibbs (1950), and it is still used to describe many magnetic WDs (see, e.g., Bagnulo et al. 2024). In this respect, magnetic WDs (MWDs) are rather similar to the small fraction ( $\sim 7\%$ ) of magnetic upper main-sequence stars (magnetic Ap, Bp and O stars: see, e.g., Donati & Landstreet 2009), which also exhibit stable magnetic fields with a typical strength of about 1–100 kG. These intrinsically stable fields are referred to as "fossil fields". That these fields exist in only a fraction of WDs and of upper main-sequence stars, that is, in settings without an obvious dynamo activity, is one of the outstanding physical puzzles of stellar evolution.

Studies of volume-limited samples of MWDs have revealed two specific evolution paths. (1) WDs resulting from single-star evolution, with typical masses of about  $0.6M_{\odot}$ , only very rarely reveal detectable fields during at least the first billion years of cooling, and the fields observed in these young WDs are almost always very weak, typically tens or hundreds of kiloGauss (kG). As the WDs cool, after about 2–3 Gyr, the fields begin to appear much more frequently and with much greater field strength (Bagnulo & Landstreet 2022). (2) The most massive WDs, with masses above perhaps  $1.1M_{\odot}$ , are probably produced by WD-WD binary mergers (Tout et al. 2008; Briggs et al. 2015; García-Berro et al. 2012). These massive WDs are usually strongly magnetic from nearly (or exactly) the moment of the merger, with

fields of many megaGauss (MG) and very short rotation periods (Bagnulo & Landstreet 2022). Intermediate-mass WDs probably represent a mixed population with a variety of origins, and may frequently result from binary evolution.

However, our observational understanding of the later evolution of magnetic fields in WDs that are older than a cooling age of about 5 Gyr is extremely limited. By this age, most magnetic WDs no longer display detectable Balmer lines (He lines disappear at a much younger age), which are commonly employed for detecting a magnetic field through spectral lines. If, however, WDs are metal polluted from accretion of circumstellar debris (often classified as DZ WDs), metal lines can be employed (Hollands et al. 2017, 2018a; Kawka et al. 2019). Alternatively, the magnetism of cool carbon-rich WDs with strong carbon-based molecular bands, classified as DQ WDs, can be studied using polarization in CH molecular bands when they are detectable e.g., Angel & Landstreet (1972), Berdyugina et al. (2007), and Vornanen et al. (2013). In the remaining featureless cool WDs, which are classified as DC WDs, a broad-band polarimetry may be employed. This technique has hardly been used for magnetic field searches since the 1970s (Angel et al. 1981). After these earliest works, the only discoveries of magnetic DC WDs were those made with spectropolarimetry by Putney (1997) and by Bagnulo & Landstreet (2020). Before the survey of magnetic WDs in the local 20 pc volume was completed (Bagnulo & Landstreet 2021), only 10 of the 30 DC WDs in this volume (the nearest and brightest DC WDs) had been searched for evidence of magnetism, and virtually none of the fainter, more distant DCs had been studied. This lack of data meant that we had almost no information about the presence of magnetic fields in the commonest spectral class of the oldest WDs. Hence, the magnetism in WDs that was produced during the first half of the age of the disk of the Milky Way was almost completely unknown territory.

In order to fill some of this information void, we are carrying out a systematic survey of optical circular polarization of known and suspected DC WDs in the northern hemisphere (Berdyugin et al. 2022, 2023). Here, we present a compilation of more than 110 new observations obtained for 84 WDs in 2022 July, 2023 November, and 2024 February with the high-precision three-band polarimeter DIPol-UF (Double Image Polarimeter - Ultra Fast) deployed at the Nordic Optical Telescope (NOT), located at the Observatorio del Roque de los Muchachos on the Canary Island of La Palma, Spain, including six new detections of magnetic DC WDs.

## 2. Observations

New broad-band circular polarization (BBCP) measurements were obtained from 2023 March – 2024 February using the DIPol-UF three-band polarimeter on the 2.5 m NOT. This instrument has been described in detail by Pirola et al. (2021). Briefly, we obtain measurements of broad-band circular polarization in three bands with DIPol-UF (which we call  $B'$ ,  $V'$ ,  $R'$ ), each about 1000 Å wide, centered on the wavelengths 4450 Å, 5400 Å, and 6400 Å. These bands are defined by sharp-cutoff dichroic filters with a transmission of about 90 % across most of each band (see Fig. 1 of Berdyugin et al. 2022). The stability, sensitivity, and zeropoint errors of DIPol-UF have been studied extensively using observations of bright standard stars and WDs with known circular polarization properties, and it is clear that we can reliably detect polarization levels down to 0.01 % with a precision and accuracy of 0.002 % at least. In practice, the precision of the survey is mainly limited by the photon number from each target

WD at a given telescope (Pirola et al. 2021; Berdyugin et al. 2022).

### 2.1. Observations of standard stars

During our observing run, we obtained measurements of various bright nonpolarized nearby stars to calibrate the instrumental polarization. In addition, we observed the well-known MWD WD 1900+705, which appears to show a signal of circular polarization that is nearly constant with time (see, e.g. Bagnulo & Landstreet 2019).

The measurements of unpolarized stars yield an instrumental polarization to a precision better than  $10^{-5}$  (a few parts per million). In the  $B'V'R'$  bands, the values of the reduced Stokes parameter  $V/I$  are  $0.0121 \pm 0.0004$  %,  $0.0109 \pm 0.0005$  %, and  $0.0084 \pm 0.0004$  %, respectively. This instrumental polarization was subtracted from the measured polarization of all targets.

### 2.2. Science targets

Most DC WDs have relatively low effective temperature  $T_{\text{eff}}$  values, often lower than 5000 K, and the nearest DC WDs mostly have *Gaia*  $G$  magnitudes of 15 or fainter. All our targets were chosen based on the recent nearly complete survey of spectral types and physical parameters of northern WDs within 40 pc of the Sun (McCleery et al. 2020; O'Brien et al. 2024). By expanding our survey to a volume within roughly 40 pc of the Sun, we reach typical magnitudes of 17 or even fainter for the most interesting (oldest) DCs. This is near or beyond our limiting magnitude for the desired measurement uncertainty level.

Table 1 gives the list of DC WDs that we observed during four observing runs on the NOT in 2022 November, 2023 March and November, and 2024 February. We also included some observations that were obtained in a previous run in July 2022, which were not published in our previous papers because of an oversight. The target names are listed according to the (frequently unofficial but convenient) Villanova designation (McCook & Sion 1977, 1999), followed by the main *Simbad* identifier, the *Gaia*  $G$  magnitude and distance, and various stellar parameters derived from Blouin et al. (2019) and Gentile Fusillo et al. (2021). The last column of Table 1 shows the spectral class of the WD when it is different than DC, using the classification by O'Brien et al. (2024) (see below). In addition to targets that were never observed before, our list includes a number of WDs in which a magnetic field has been detected in previous studies, namely WD 0004+122 (Bagnulo & Landstreet 2020); WD 0548–001 (spectral class: DQp Landstreet & Angel 1971); WD 0756+437 (Putney 1997); WD 1008+290 (spectral class: DQ, Schmidt et al. 1999); WD 1036–204 (spectral class: DQ, Liebert et al. 1978); WD 1315+222 (Berdyugin et al. 2022); WD 1346+121 (Berdyugin et al. 2023); WD 1556+044 (Berdyugin et al. 2022); WD 2049–222 (Berdyugin et al. 2022); WD 2049–253 (Bagnulo & Landstreet 2020); WD 2211+372 (Berdyugin et al. 2023). These observations served to confirm detection, to further verify the instrument reliability and stability, and to set a baseline for future studies of the rotational periods of these MWDs.

This target list includes different categories of cool WDs: He-rich and H-rich featureless WDs, and a small number of cool DQ WDs with molecular carbon ( $C_2$ ) bands. WDs with He-rich atmospheres cease to display spectral lines when the cooling has reduced  $T_{\text{eff}}$  below about 11 000 K, which occurs at a cooling age of about 1 Gyr, and our list includes a number of DC WDs of this

type that have ages of only 2–4 Gyr. In contrast, the Balmer lines of WDs with H-rich atmospheres are still visible until  $T_{\text{eff}}$  has dropped to a value of about 5000 K, which requires a cooling time of about 5 Gyr.

The resulting measurements of the broad-band circular polarization in each of the three filter bands, together with timing information, including JD, date, and time at the middle of each observation, and the total exposure time of each target, are listed in Table 2. Each observation consisted of a long series of 30s to 60s exposures. We report in Table 2 the average of these series values, hereafter called measurements, while the mean quadratic error from the individual exposures of a given series was used to estimate the measurement error. Additional details of the data acquisition and reduction are discussed in Berdyugin et al. (2022).

Inspection of Table 2 shows that for the hotter targets, the uncertainties tend to be similar across all three bands, and they tend to be smallest in the red  $R'$  band for the cooler WDs. For obvious reasons, the uncertainties are larger for the fainter WDs, for which they sometimes rise above 0.1%. Single-filter measurements that show a detection of a nonzero circular polarization at the  $3\sigma$  level or better are indicated in Table 2 by boldface fonts. We considered that we detected nonzero circular polarization either (1) when more than one measurement in any filter band exceeded a significance of  $3\sigma$ , or (2) when a single measurement was obtained with a significance of  $5\sigma$ . With these criteria, we detected fields in 6 of the 75 new WDs reported in this study. These stars are indicated by boldface fonts for their names in Tables 1 and 2. Two of the six fields we detected were further confirmed by the detection of similar polarization levels in two successive measurements. The names of the new magnetic WDs discovered in this survey are highlighted with an asterisk in Tab. 2.

### 3. Results

#### 3.1. Newly discovered magnetic WDs

Among the stars that were observed for the first time in this survey, we detected a nonzero signal of circular polarization in six WDs: WD 0004+337 = LP 240-29; WD 0019+423 = EGGR 459; WD 0021+683 = G 242-54B; WD 0419+576 = LP 84-16; WD 06542+059 = 2MASS J06572938+0550479; and WD 0745+115 = SDSS J074842.48+112502.0. Their polarization as a function of the broad-band filters is shown in Fig. 1. We comment on the newly discovered stars below. In addition, we comment on the known very strong field MWD WD 0745+115, which shows short-term variability.

##### 3.1.1. WD 0004+337

This WD was originally identified by Luyten (1995) as a nearby object based on its high proper motion. It was classified as a probable DC WD by Limoges et al. (2015) and was confirmed using *Gaia* data by Gentile Fusillo et al. (2019, 2021). Spectral class DC and physical parameters were determined by Blouin et al. (2019). Most recently, the physical parameters have been slightly revised by O'Brien et al. (2024). Because  $T_{\text{eff}}$  is significantly above 5000 K without any trace of H $\alpha$ , it is assumed to have a He-rich atmosphere. The cooling age of this DCH star is estimated to be nearly 5 Gyr (the letter H after the spectral type DC means that the WD is magnetic).

We only observed this WD once, but nonzero polarization at about the 0.5% level was observed in the  $B'$  filter at the  $9\sigma$

level and in the  $R'$  filter at the  $8\sigma$  level. We therefore regard this detection as quite secure. The polarization detected in both filters has the same sign. However, remarkably, a barely detectable polarization level (at  $3\sigma$ ) was observed in the  $V'$  filter.

##### 3.1.2. WD 0019+423

This object, first identified as a WD by Greenstein (1979), has been included in numerous studies. Its parameters have most recently been derived by O'Brien et al. (2024), who considered it to have a DC spectrum with a He-rich atmosphere. However, with a derived mass of only  $0.39M_{\odot}$ , which is slightly below the lowest mass that can be produced by single-star evolution, we suspect that this object may be an undetected binary pair of two similar WDs.

Circular polarization is detected at roughly the 0.8% level only in the  $B'$  band, but the observed values are nonzero at the  $12\sigma$  levels, and the detection is therefore very secure. If our suspicion of binarity is correct and roughly half the light is contributed by a nonpolarized WD, the typical polarization levels in the two bands showing clear nonzero polarization could be near the 1.6% level. In any case, the broad-band variation of the polarization is rather similar to that of WD 0004+337 above.

##### 3.1.3. WD 0021+683

This WD is the fainter member of a common-proper-motion binary with a separation of about 5 arcsec. The companion is a very cool star some three mag brighter than the WD, presumably an M dwarf. The object was identified as a WD by Gentile Fusillo et al. (2019) and was observed spectroscopically by Tremblay et al. (2020). It is included in the 40 pc WD sample (McCleery et al. 2020; O'Brien et al. 2024). It appears to have a He-rich atmosphere and an age of more than 5 Gyr.

Circular polarization is only detected with high confidence in the  $R'$  band, where the polarization of 0.435% provides a detection at nearly the  $6\sigma$  level. Polarization is also detected in the  $V'$  band at the  $3.5\sigma$  level, so that the field in this star is considered to be reliably detected, but is close to the threshold for a reliable detection with our telescope and instrument.

This WD shows only weak polarization in the  $B'$  band and appears to have a BBCP spectrum that changes sign at a wavelength between the  $R'$  band and the two bluer bands.

##### 3.1.4. WD 0419+576

This object is a relatively warm DC WD with a cooling age of about 2.5 Gyr. It was identified as a WD candidate from the *Gaia* DR2 data (Jiménez-Esteban et al. 2018). A spectrum obtained by Tremblay et al. (2020) led to a clear identification as a DC WD. The WD is within the 40 pc volume (McCleery et al. 2020; O'Brien et al. 2024).

The absolute value of the observed circular polarization signal is consistently about 0.15% in the three bands, but it changes sign between the  $B'$  and the other two bands. In the  $B'$  and  $V'$  bands, the signal is only detected at about the  $3\sigma$  level, but in the  $R'$  band, the detection is at the  $5\sigma$  level, and we consider that the detection of a field is secure, if uncomfortably close to our detection limit. The magnetic field of this DCH star is probably somewhat weaker than those of the three WDs discussed above.

### 3.1.5. WD 0654+059

This object is a recently discovered nearby WD. It was first identified in the *Gaia* DR2 release by Jiménez-Esteban et al. (2018). The WD is located within the local 40 pc volume, and the physical parameters were estimated by Gentile Fusillo et al. (2019, 2021); McCleery et al. (2020); O’Brien et al. (2024). A flux spectrum was obtained by Tremblay et al. (2020), which resulted in the DC classification.

Three band polarization measurements were obtained during two winter runs. Polarization was clearly detected first in one band and then in two bands, and finally (by substantially increasing the total time on target), in all three bands. However, a close examination of the measured polarization values obtained during the three measurements does not reveal any clear temporal variation between them within the measurement errors. It appears that all three bands report polarization values of the same sign, but the  $V'$ -band polarization value is higher by about 50 % than the values found in the other two bands. The highest Stokes  $V/I$  value we found is just below 0.5 %.

### 3.1.6. WD 0745+115

Like several of the targets in this section, WD 0745+115 is a very recent addition to the list of relatively nearby WDs, although it lies outside the 40 pc volume. It was identified as a nearby WD by Jiménez-Esteban et al. (2018), an identification confirmed by Gentile Fusillo et al. (2019). A spectrum was obtained by Kilic et al. (2020), who identified the WD as a DC star. The basic parameters were derived by Gentile Fusillo et al. (2019, 2021), who reported that it has a relatively high mass of  $0.93 M_{\odot}$  and an effective temperature  $T_{\text{eff}}$  close to  $10^4$  K. For this WD, the absence of Balmer lines is a very clear indication of a He-rich atmosphere.

Strong circular polarization is present in all observed bands. The polarization approaches +2% in the  $V'$  band, is close to +1% in the  $R'$  band, and reverses sign and exceeds -1% in the  $B'$  band. There is no significant indication of variability in the four measurements taken during about one year.

### 3.1.7. WD 0756+437

WD 0756+437 was observed as an extremely interesting target of opportunity that was easily included in our general program. The star was originally identified as a DF-C WD with a possible  $\lambda 4670 \text{ \AA}$  feature (Greenstein et al. 1977; Greenstein 1979). It was repeatedly observed photometrically and spectroscopically since then, especially after the polarimetric discovery of a large magnetic field (see below). Putney (1995) identified the object as a DA WD with a H-rich atmosphere on the basis of the comparison of features in the polarization spectrum with the theoretical spectrum of H. The star is within the 40 pc volume around the Sun (McCleery et al. 2020; O’Brien et al. 2024).

An extremely high level of circular polarization that rises to the huge value of  $V/I \sim 8\%$  at around  $5500 \text{ \AA}$  was discovered by Putney (1995), who published a single (nearly featureless) flux spectrum and an excellent circular polarization spectrum. The observed polarization level indicates that this WD possesses a very strong field. Our broad-band Stokes  $V/I$  measurements are fully consistent with Putney’s data.

Putney compared narrow polarization features with predicted wavelength positions of various components of  $H\alpha$  in fields of hundreds of MG (Wunner et al. 1985) and concluded that the mean ( $\langle |B| \rangle$ ) field must be about 200–220 MG in strength. This

field strength was also supported by Schmidt et al. (2003) on the basis of SDSS intensity spectra. Comparison of the spectral energy distribution with models (Limoges et al. 2015; Gentile Fusillo et al. 2021) suggests that  $T_{\text{eff}} = 7215 \text{ K}$ ,  $M = 1.04 M_{\odot}$ , and that the cooling age is about 4.45 Gyr. This DAH WD is thus probably (one of?) the oldest known, strongly magnetized products of a WD-WD merger (García-Berro et al. 2012; Bagnulo & Landstreet 2022).

We took five polarization data sets during two years. From the fact that the first two measurements, taken about 3 hr apart, also provide the largest and smallest polarization values in our measurement set, we deduce that the rotation period of this star could be of the order of six hours. Photometry by Brinkworth et al. (2013) showed very large amplitude sinusoidal photometric variations (semi-amplitude of  $\pm 4\%$ ) with a unique period of 6.68 hr. Because the polarimetric variations are due to and locked to the stellar rotation, the agreement of the polarimetric period constraints with the photometric period confirms that the photometric period is the stellar rotation period.

## 3.2. Other targets with marginal detections

In addition to these reasonably certain detections, the observations of nine other DC WDs provided a single detection at or slightly above the  $3\sigma$  level in one band. These WDs can be regarded as candidates that need further measurements for a confirmation (for these targets, only the significant detections, but not the names, are shown in boldface in Table 2). They are WD 0052+595; WD 0102+210; WD 0156+155; WD 0357+513; WD 0407+197; WD 0426+588; WD 1554-079; WD 1731+290. Because of previous experience with unsuccessfully trying to confirm magnetic fields based on a single  $3\sigma$  polarization detection (see Sect. 3.3 below), we suspect that the majority of these detections will not be confirmed, except perhaps for the case of WD 0052+595.

## 3.3. Targets with unconfirmed detections

In our previous observing runs, polarization was detected once in a single band at a level slightly higher than  $3\sigma$  in observations of WD 1434+437 and WD 1533+469 (Berdyugin et al. 2023). We obtained one more observation of each of these two stars that failed to confirm the marginal detections reported earlier. We dropped these stars from our list of DCH candidates.

## 4. Discussion and conclusions

The circular polarization levels detected with the DIPoL-UF at NOT range from about 1 %, found in two DC WDs to a number of detections of polarization at levels between 0.2 % and 0.6 %, with measurement uncertainties ranging between about 0.02 % to 0.1 %. It is clear that an extremely important feature of the DIPoL-UF polarimeter is its stable and precisely measured zero-point (Berdyugin et al. 2022). However, our observing program reaches the limit of what can be achieved with a medium-sized telescope such as the 2.5 m NOT. Further substantial progress will require the use of larger telescopes.

Figure 2 shows the relation of the magnitude and the uncertainty of our measurement errors of all NOT+DIPoL-UF measurements of WDs as a function of *Gaia*  $G$  magnitude, normalized to 1 h exposure time. This figure represents a substantial update compared to Fig. 4 of Berdyugin et al. (2022). It may be used to make quantitative predictions regarding the level of

polarimetric precision that may be achieved for the BBCP measurements as a function of exposure time and stellar magnitude. It can also be used to evaluate observational requirements for a given WD with DIPOL-UF employed on a larger telescope.

Our search for broad-band circular polarization, and therefore, for magnetic fields, in DC WDs continues to deliver detections of previously unknown fields in these faint and featureless objects, with a detection rate of 13 new MWDs so far out of 101 observed new targets. The diverse outcome obtained in our different runs is remarkable: Berdyugin et al. (2022) reported the detection of 2 new MWDs out of 3 newly observed DC WDs, Berdyugin et al. (2023) reported 5 out of 23, and we detected and reported 6 new MWDs out of 75. Overall, the detection of a magnetic field in 13 out of 105 observed WDs is fully consistent with the frequency of the occurrence of magnetic fields in the DC WDs in the local 20 pc volume,  $13.3 \pm 6.2\%$ , that was measured by Bagnulo & Landstreet (2021). This value is certainly an underestimate of the actual frequency of magnetic fields in old WDs because stars with magnetic fields weaker than a few MG do not produce a signal of circular polarization that can be detected with our instruments. On the other hand, only 2 of the newly discovered magnetic DC stars show circular polarization levels in excess of 1%. We found no new magnetic DC WDs with extremely high polarization levels in our survey (several percent polarization), similar to those found in other types of magnetic WDs, such as WD 1900+705 (=Grw+70° 8247, 3%), WD 0756+437 (=EGGR 428, ~ 8% Kemp et al. 1970), CL Oct (=EUVE J0317–85.5, ~ 11% Barstow et al. 1995), and WD 1031+234 (=PG 1031+234, ~ 12% West & Schmidt 1984; Latter et al. 1986; Schmidt et al. 1986). Our new data, combined with spectropolarimetric surveys of WDs of various cooling ages, will eventually help us to understand the origin and evolution of magnetic fields in degenerate stars.

We note that roughly half of the DCs observed in this survey belong to the category of younger DCs that have He atmospheres,  $T_{\text{eff}} \gtrsim 6000$  K, and cooling ages younger than about 4 Gyr. These stars were presumably DB WDs earlier in their cooling. The other, older, DCs, also half of the sample, with lower  $T_{\text{eff}}$  values and ages older 4 or 5 Gyr, may have H-rich or He-rich atmospheres, and these stars sample the production of magnetic WDs during the first few billion years of the evolution of the Milky Way galaxy.

We cannot assign definite magnetic field strengths to the observed polarization signals because the theory of continuum circular polarization in these very cool WDs has not been studied in detail. However, using a rough estimate (derived from somewhat hotter magnetic WDs) that polarization  $V/I \sim 1\%$  is produced by a mean line-of-sight field component  $\langle B_z \rangle$  of about 15 MG (Bagnulo & Landstreet 2020), most of the fields detected in our survey probably have overall typical field strengths  $\langle |B| \rangle$  of a few MG to tens of MG, rising to perhaps as high as 100 MG in the most highly polarized WDs.

The magnetic fields of DC WDs has been an almost completely neglected topic since the 1970s, when searches with broad-band polarimetry went out of fashion. We showed that this method of searching for fields in these generally faint WDs is still an extremely powerful tool that has revealed MG-level fields in a significant fraction of the DCs. These newly discovered magnetic DC WDs can now be studied with spectropolarimetry using larger telescopes, which will provide additional constraints for developing a suitable model for their enigmatic circularly polarized continuum spectra.

*Acknowledgements.* Based on observations made with the Nordic Optical Telescope, owned in collaboration by the University of Turku and Aarhus University,

and operated jointly by Aarhus University, the University of Turku and the University of Oslo, representing Denmark, Finland and Norway, the University of Iceland and Stockholm University at the Observatorio del Roque de los Muchachos, La Palma, Spain, of the Instituto de Astrofísica de Canarias. DIPOL-UF is a joint effort between University of Turku (Finland) and Leibniz Institute for Solar Physics (Germany). We acknowledge support from the Magnus Ehrnrooth foundation and the ERC Advanced Grant HotMol ERC-2011-AdG-291659. JDL acknowledges the financial support of the Natural Sciences and Engineering Research Council of Canada (NSERC), funding reference number 6377-2016.

## References

- Angel, J. R. P., Borra, E. F., & Landstreet, J. D. 1981, *ApJS*, 45, 457  
 Angel, J. R. P. & Landstreet, J. D. 1972, *ApJ*, 178, L21  
 Bagnulo, S., Farihi, J., Landstreet, J. D., & Folsom, C. P. 2024, *ApJ*, 963, L22  
 Bagnulo, S. & Landstreet, J. D. 2019, *MNRAS*, 486, 4655  
 Bagnulo, S. & Landstreet, J. D. 2020, *A&A*, 643, A134  
 Bagnulo, S. & Landstreet, J. D. 2021, *MNRAS*, 507, 5902  
 Bagnulo, S. & Landstreet, J. D. 2022, *ApJ*, 935, L12  
 Barstow, M. A., Jordan, S., O'Donoghue, D., et al. 1995, *MNRAS*, 277, 971  
 Bédard, A., Bergeron, P., Brassard, P., & Fontaine, G. 2020, *ApJ*, 901, 93  
 Berdyugin, A. V., Pirola, V., Bagnulo, S., Landstreet, J. D., & Berdyugina, S. V. 2022, *A&A*, 657, A105  
 Berdyugin, A. V., Pirola, V., Bagnulo, S., Landstreet, J. D., & Berdyugina, S. V. 2023, *A&A*, 670, A2  
 Berdyugina, S. V., Berdyugin, A. V., & Pirola, V. 2007, *Phys. Rev. Lett.*, 99, 091101  
 Blouin, S., Dufour, P., Thibeault, C., & Allard, N. F. 2019, *ApJ*, 878, 63  
 Briggs, G. P., Ferrario, L., Tout, C. A., Wickramasinghe, D. T., & Hurley, J. R. 2015, *MNRAS*, 447, 1713  
 Brinkworth, C. S., Burleigh, M. R., Lawrie, K., Marsh, T. R., & Knigge, C. 2013, *ApJ*, 773, 47  
 Donati, J.-F. & Landstreet, J. D. 2009, *ARA&A*, 47, 333  
 Ferrario, L., Wickramasinghe, D., & Kawka, A. 2020, *Advances in Space Research*, 66, 1025  
 García-Berro, E., Lorén-Aguilar, P., Aznar-Siguán, G., et al. 2012, *ApJ*, 749, 25  
 Gentile Fusillo, N. P., Tremblay, P. E., Cukanovaite, E., et al. 2021, *MNRAS*, 508, 3877  
 Gentile Fusillo, N. P., Tremblay, P.-E., Gänsicke, B. T., et al. 2019, *MNRAS*, 482, 4570  
 Greenstein, J. L. 1979, *ApJ*, 227, 244  
 Greenstein, J. L., Oke, J. B., Richstone, D., van Altena, W. F., & Steppe, H. 1977, *ApJ*, 218, L21  
 Hollands, M. A., Gänsicke, B. T., & Koester, D. 2018a, *MNRAS*, 477, 93  
 Hollands, M. A., Koester, D., Alekseev, V., Herbert, E. L., & Gänsicke, B. T. 2017, *MNRAS*, 467, 4970  
 Hollands, M. A., Tremblay, P.-E., Gänsicke, B. T., Gentile-Fusillo, N. P., & Toonen, S. 2018b, *MNRAS*, 480, 3942  
 Jiménez-Esteban, F. M., Torres, S., Rebassa-Mansergas, A., et al. 2018, *MNRAS*, 480, 4505  
 Kawka, A., Vennes, S., Ferrario, L., & Paunzen, E. 2019, *MNRAS*, 482, 5201  
 Kemp, J. C., Swedlund, J. B., Landstreet, J. D., & Angel, J. R. P. 1970, *ApJ*, 161, L77  
 Kilic, M., Bergeron, P., Kosakowski, A., et al. 2020, *ApJ*, 898, 84  
 Landstreet, J. D. & Angel, J. R. P. 1971, *ApJ*, 165, L67  
 Latter, W. B., Schmidt, G. D., & Green, R. F. 1986, in *Bulletin of the American Astronomical Society*, Vol. 18, 975  
 Liebert, J., Angel, J. R. P., Stockman, H. S., & Beaver, E. A. 1978, *ApJ*, 225, 181  
 Limoges, M. M., Bergeron, P., & Lépine, S. 2015, *ApJS*, 219, 19  
 McCleery, J., Tremblay, P.-E., Gentile Fusillo, N. P., et al. 2020, *MNRAS*, 499, 1890  
 McCook, G. P. & Sion, E. M. 1977, *A Catalogue of spectroscopically identified white dwarfs*  
 McCook, G. P. & Sion, E. M. 1999, *ApJS*, 121, 1  
 O'Brien, M. W., Tremblay, P. E., Klein, B. L., et al. 2024, *MNRAS*, 527, 8687  
 Pirola, V., Kosenkov, I. A., Berdyugin, A. V., Berdyugina, S. V., & Poutanen, J. 2021, *AJ*, 161, 20  
 Putney, A. 1995, *ApJ*, 451, L67  
 Putney, A. 1997, *ApJS*, 112, 527  
 Saumon, D., Blouin, S., & Tremblay, P.-E. 2022, *Phys. Rep.*, 988, 1  
 Schmidt, G. D., Harris, H. C., Liebert, J., et al. 2003, *ApJ*, 595, 1101  
 Schmidt, G. D., Liebert, J., Harris, H. C., Dahn, C. C., & Leggett, S. K. 1999, *ApJ*, 512, 916  
 Schmidt, G. D., West, S. C., Liebert, J., Green, R. F., & Stockman, H. S. 1986, *ApJ*, 309, 218  
 Stibbs, D. W. N. 1950, *MNRAS*, 110, 395  
 Tout, C. A., Wickramasinghe, D. T., Liebert, J., Ferrario, L., & Pringle, J. E. 2008, *MNRAS*, 387, 897  
 Tremblay, P. E., Hollands, M. A., Gentile Fusillo, N. P., et al. 2020, *MNRAS*, 497, 130  
 Vornanen, T., Berdyugina, S. V., & Berdyugin, A. 2013, *A&A*, 557, A38  
 West, S. C. & Schmidt, G. D. 1984, in *Bulletin of the American Astronomical Society*, Vol. 16, 945  
 Wunner, G., Roesner, W., Herold, H., & Ruder, H. 1985, *A&A*, 149, 102

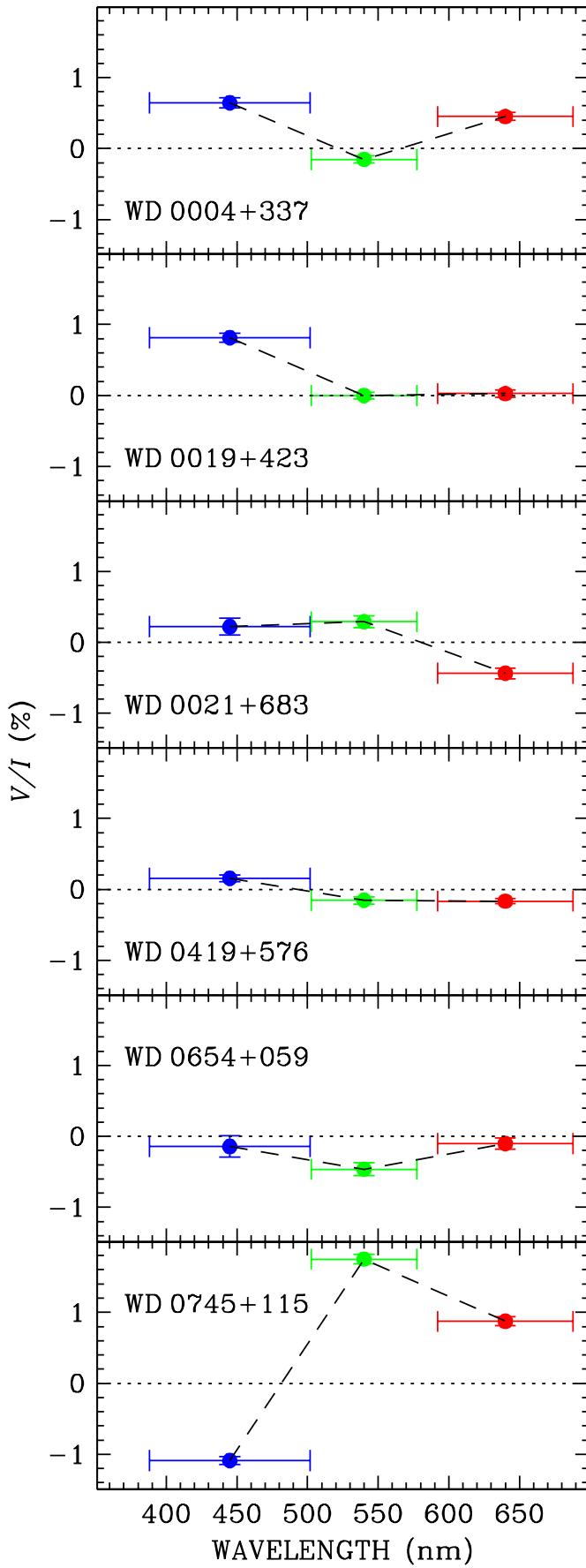


**Fig. 1.** Wavelength dependence of the circular polarization for the six newly detected magnetic WDs.

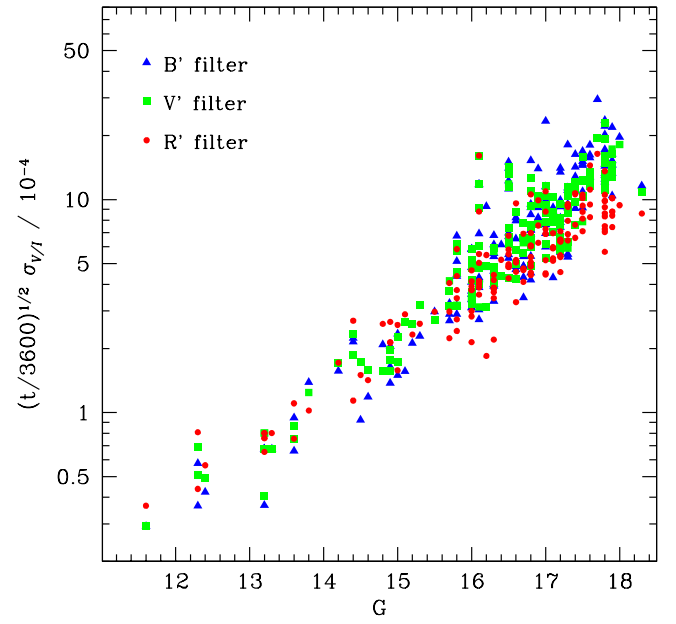


**Fig. 2.** Relation of the magnitude and measurement errors of all DIPoL-UF measurements of WDs at NOT as a function of *Gaia* *G* magnitude, normalized to 1 h exposure time.

**Table 1.** Basic parameters of stars observed.

STAR	$G$	$d$ (pc)	$T_{\text{eff}}$ (K)	$M$ ( $M_{\odot}$ )	Age (Gyr)	Atmosphere	
<b>WD 0004+122</b>	LP 464-57	16.3	17.5	5223	0.76	7.614	H
<b>WD 0004+337</b> *	LP 240-29	17.2	34.9	5792	0.76	4.923	He
WD 0019+264	LP 349-1	17.5	32.9	4991	0.58	5.974	H
<b>WD 0019+423</b> *	EGGR 459	16.4	34.5	5625	0.39	2.055	He
<b>WD 0021+683</b> *	G 242-54B	17.5	36.0	5644	0.73	5.578	He
WD 0034-285	2MASS J00371373-2814503	17.6	37.7	5472	0.72	5.557	H
WD 0052+595	LSPM J0055+5948	16.8	22.8	4645	0.48	5.694	H
WD 0102+210	EGGR 463	17.8	32.5	4721	0.62	8.125	H
WD 0156+155	PG 0156+156	15.8	38.2	9507	0.76	1.132	He
WD 0158+119	GD 21	16.1	31.5	7224	0.68	1.926	He
WD 0200-127	GD 1072	14.5	24.1	10261	0.76	0.916	He
WD 0222+647	LP 53-7	17.9	31.0	4189	0.47	7.07	H
WD 0228+079	LP 530-21	17.2	38.9	5850	0.60	3.322	He
WD 0230+212	LP 410-52	17.2	28.5	4730	0.50	5.60	H
WD 0306+663	LSR J0310+6634	17.9	38.4	4681	0.47	5.269	H
WD 0313+393	GD 44	15.7	37.9	9162	0.72	1.123	He
WD 0315+423	UCAC4 663-016444	14.8	30.6	11260	0.76	0.719	He (DBA)
WD 0317+233	LP 355-59	17.6	39.8	4690	0.40	3.941	H
WD 0342-039	2MASS J03450153-0348492	17.8	31.0	4362	0.49	6.907	H
WD 0344+014	LP 593-56	16.3	20.2	4959	0.51	4.530	H
WD 0357+513	LSR J0401+5131	17.1	25.1	5018	0.69	6.975	He
WD 0359+153	2MASS J04024236+1527419	16.6	36.9	7145	0.75	2.653	He
WD 0407+197	LP 414-106	17.5	29.1	4965	0.69	8.200	H
<b>WD 0419+576</b> *	LP 84-16	16.6	37.4	7439	0.77	2.473	He
WD 0426+588	EGGR 180	12.3	5.5	7294	0.72	2.187	He
WD 0431+308	LP 302-33	17.8	34.1	4764	0.60	7.658	H
WD 0535+438	LP 203-56	17.3	39.3	5961	0.67	3.872	He
WD 0541+260	LSR J0544+2603	16.9	36.0	4778	0.26	2.192	H
WD 0543+112	LSPM J0546+1115	17.7	36.5	4870	0.53	5.483	H
<b>WD 0548-001</b>	EGGR 248	14.4	11.2	6053	0.65	3.35	He (DQ)
WD 0549-261	2MASS J05511869-2609125	17.2	39.6	4752	0.27	2.373	H
WD 0638-044	PM J06411-0432	17.0	20.4	4062	0.45	7.092	H
<b>WD 0654+059</b> *	2MASS J06572938+0550479	17.3	39.0	6010	0.69	3.961	He
WD 0714+458	GD 84	15.2	35.5	10314	0.67	0.751	He
WD 0726+536	LP 123-5	17.9	36.2	4589	0.51	6.573	H
<b>WD 0745+115</b> *	GALEX J074842.4+112502	16.5	46.7	9831	0.93	1.708	He
WD 0748+614	GD 453	16.0	35.0	8270	0.74	1.536	He
WD 0749+426	LP 207-50	17.2	27.4	4585	0.47	5.576	H
WD 0751+578	G 193-78	15.0	29.4	10011	0.76	0.980	He
<b>WD 0756+437</b>	EGGR 428	16.1	22.0	7215	1.04	4.450	H
WD 0759-283	Gaia DR3 5597759970724418688	16.8	35.0	5682	0.48	2.502	He (DQp)
WD 0810+489	G 111-64	14.9	17.1	6709	0.65	2.17	He
WD 0847-017	LP 606-12	17.1	27.9	4884	0.54	5.727	H
WD 0848+166	LP 426-17	16.6	30.9	5907	0.59	3.024	He
WD 0853-083	PM J08555-0833	17.6	33.1	4579	0.46	5.544	H
WD 0900+734	G 252-27	16.8	25.7	5065	0.53	5.09	He
WD 0945+206	LP 428-41	17.8	37.2	4909	0.58	6.401	H
WD 0947+153	LP 428-53	17.4	39.2	5320	0.51	3.950	He
WD 0958+436	SDSS J100204.08+432645.6	17.8	34.9	4699	0.52	6.251	H
<b>WD 1008+290</b>	LP 315-42	16.5	14.7	3962	0.41	5.991	He (DQp)
WD 1012+083	LP 549-32	17.5	29.5	4558	0.50	6.395	H
<b>WD 1036-204</b>	EGGR 535	15.8	14.1	5754	0.94	6.185	He (DQp)
WD 1037+103	PM J10403+1004	17.1	36.9	5983	0.65	3.614	He
WD 1049+411	LP 213-79	16.7	33.9	6237	0.64	2.815	He
WD 1055-072	LAWD 34	14.2	12.3	7388	0.81	2.822	He
WD 1122+214	LP 374-46	16.9	38.1	6194	0.60	2.410	He
WD 1143+633	EGGR 353	16.2	24.0	5484	0.53	2.589	H (DA)
WD 1153+135	LP 493-78	17.4	35.6	4769	0.42	3.740	H
WD 1155+003	LSPM J1158+0004	17.9	34.6	4415	0.46	6.182	H

Table 1. continued.

	STAR	$G$	$d$ (pc)	$T_{\text{eff}}$ (K)	$M$ ( $M_{\odot}$ )	Age (Gyr)	Atmosphere
WD 1223+188	LP 435-109	16.2	35.9	7972	0.80	2.031	H (DAHe)
WD 1239-133	EC 12393-1318	15.7	35.9	8643	0.68	1.196	He
WD 1245-102	2MASS J12482817-1028576	16.8	39.7	7398	0.82	2.854	He
WD 1310+027	LP 557-24	17.9	30.9	4165	0.47	7.154	H
<b>WD 1315+222</b>	LP 378-956	16.7	31.8	6334	0.72	3.541	He
WD 1343+422	LP 219-63	17.0	37.5	4639	0.24	2.270	H
<b>WD 1346+121</b>	LP 498-66	17.8	28.3	4435	0.63	9.231	H
WD 1419+426	PB 2202	17.3	45.8	8901	1.12	3.236	H (DA)
WD 1434+437	LP 221-217	17.2	27.2	4634	0.49	5.886	H
WD 1533+469	LP 176-60	17.8	30.8	4309	0.47	6.678	H
WD 1547+572	LP 99-578	17.3	37.9	5770	0.67	4.567	He
WD 1554-079	NAME SSS J1556-0806	18.3	32.7	7155	1.29	2.712	He
<b>WD 1556+044</b>	PM J15589+0417	16.0	22.5	6867	0.91	4.218	H
WD 1717+104	2MASS J17200675+1022278	17.6	37.6	4973	0.51	5.122	He
WD 1731+290	LSPM J1733+2903	17.0	39.6	6458	0.69	2.961	He
WD 1741+145	LSPM J1743+1434S	14.9	34.3	10572	0.60	0.598	He
WD 1745+290	LSPM J1747+2859	17.5	36.6	4832	0.45	3.974	H
<b>WD 2049-223</b>	LP 872-48	14.9	20.3	8145	0.78	1.904	He
<b>WD 2049-252</b>	UCAC4 325-215293	16.0	18.0	4908	0.49	4.540	H
<b>WD 2211+372</b>	LP 287-35	16.8	29.2	6424	0.88	4.379	He
WD 2228+226	2MASS J22305914+2254543	17.0	31.0	5774	0.70	4.841	He
WD 2303+391	LSPM J2305+3922	17.9	35.9	7021	1.17	3.806	He
WD 2345+027	LP 643-65	16.6	25.2	4994	0.47	3.520	H
WD 2359+636	LSR J0002+6357	17.0	26.3	4879	0.54	5.811	H

Detections are marked in boldface. Newly discovered magnetic WDs are marked with a \*. All stars for which no spectral type is explicitly given in the last column have a featureless spectrum (spectral class DC).

Chemical composition of the stellar atmosphere was taken from O'Brien et al. (2024), temperature and mass from Gentile Fusillo et al. (2021), and ages were interpolated using the tables of Bédard et al. (2020).



**Table 2.** Observing log of WDs. Detections are marked in boldface. Newly discovered magnetic stars are marked with a \*.

STAR	DATE yyyy-mm-dd	UT hh:mm	JD – 2400000	Exp. (s)	V/I (%)		
					<i>B'</i>	<i>V'</i>	<i>R'</i>
<b>WD 0004+122</b>	2022-07-01	04:42	59761.696	3120	<b>0.813±0.060</b>	<b>0.761±0.052</b>	<b>1.268±0.037</b>
	2022-07-06	02:36	59766.608	3360	<b>0.838±0.056</b>	<b>0.676±0.042</b>	<b>1.181±0.038</b>
	2022-11-20	23:27	59904.477	3200	<b>0.982±0.049</b>	<b>0.731±0.063</b>	<b>1.201±0.047</b>
	2023-11-16	22:16	60265.428	3120	<b>0.814±0.066</b>	<b>0.794±0.051</b>	<b>1.187±0.045</b>
<b>WD 0004+337 *</b>	2023-11-17	20:25	60266.351	4800	<b>0.644±0.070</b>	<b>-0.154±0.050</b>	<b>0.451±0.056</b>
WD 0019+264	2022-11-21	20:43	59905.364	4400	0.154±0.086	-0.053±0.062	0.027±0.069
<b>WD 0019+423 *</b>	2023-11-17	22:16	60266.405	3120	<b>0.814±0.066</b>	0.000±0.047	0.026±0.049
<b>WD 0021+683 *</b>	2023-11-19	20:33	60268.356	5600	0.222±0.118	<b>0.292±0.083</b>	<b>-0.435±0.075</b>
WD 0034–285	2023-11-18	20:41	60267.362	5600	0.283±0.126	0.015±0.101	<b>-0.364±0.116</b>
WD 0052+595	2022-11-19	00:15	59902.512	4160	0.039±0.077	<b>-0.298±0.099</b>	<b>-0.203±0.063</b>
	2022-11-21	22:09	59905.423	3840	-0.045±0.086	-0.028±0.067	0.080±0.041
	2023-11-16	23:46	60265.490	5440	0.067±0.124	-0.014±0.103	<b>0.291±0.086</b>
WD 0102+210	2022-11-21	00:58	59904.540	6240	-0.002±0.174	0.247±0.169	<b>-0.234±0.068</b>
	2023-11-18	22:35	60267.441	6000	-0.134±0.091	0.175±0.092	0.018±0.068
WD 0156+155	2024-02-05	21:22	60346.390	2400	-0.044±0.039	-0.030±0.070	<b>0.193±0.046</b>
WD 0158+119	2022-11-19	01:29	59902.563	3120	0.073±0.044	0.065±0.042	-0.106±0.042
WD 0200–127	2024-02-04	20:25	60345.351	1200	0.044±0.016	-0.015±0.030	0.003±0.026
WD 0222+647	2022-11-21	23:53	59905.495	6240	0.089±0.159	0.199±0.098	-0.104±0.074
WD 0228+079	2023-11-17	23:03	60266.461	4800	-0.104±0.049	0.002±0.053	-0.029±0.047
WD 0230+212	2022-11-20	02:20	59903.597	5200	<b>-0.342±0.112</b>	-0.119±0.068	0.024±0.053
WD 0306+663	2023-11-19	01:59	60267.582	6400	0.095±0.109	0.089±0.123	0.044±0.076
WD 0313+393	2023-11-17	01:20	60265.556	3360	-0.053±0.030	-0.000±0.043	0.017±0.042
WD 0315+423	2022-11-20	03:28	59903.645	1760	-0.024±0.028	-0.031±0.021	0.032±0.035
WD 0317+233	2024-02-06	21:19	60347.388	6240	-0.349±0.123	-0.120±0.102	-0.123±0.072
WD 0342–039	2024-02-07	21:19	60348.388	6240	0.224±0.168	0.042±0.087	-0.010±0.075
WD 0344+014	2022-11-19	02:32	59902.606	3120	0.019±0.068	0.072±0.057	-0.022±0.038
	2022-11-19	03:54	59902.663	4800	-0.114±0.078	-0.031±0.087	<b>-0.161±0.050</b>
WD 0359+153	2023-11-19	00:13	60267.509	3840	0.054±0.047	-0.049±0.041	-0.044±0.049
WD 0407+197	2022-11-20	04:45	59903.698	5280	<b>0.546±0.133</b>	0.170±0.125	-0.015±0.083
	2022-11-21	03:01	59904.626	5280	0.040±0.119	-0.227±0.096	-0.026±0.080
<b>WD 0419+576 *</b>	2023-11-18	00:30	60266.521	3600	<b>0.157±0.047</b>	<b>-0.154±0.050</b>	<b>-0.165±0.033</b>
WD 0426+588	2024-02-06	22:34	60347.440	1200	<b>-0.042±0.010</b>	0.007±0.012	0.028±0.014
WD 0431+308	2023-11-20	02:14	60268.593	5600	-0.423±0.162	0.337±0.128	-0.317±0.109
WD 0535+438	2023-03-24	21:37	60028.401	5040	-0.107±0.075	-0.027±0.071	-0.056±0.065
WD 0541+260	2023-03-23	21:37	60027.401	3960	0.042±0.124	-0.102±0.085	-0.020±0.067
WD 0543+112	2023-03-26	21:41	60030.404	5600	-0.000±0.223	-0.160±0.147	0.081±0.124
<b>WD 0548–001</b>	2023-03-25	21:00	60029.375	1440	<b>-0.407±0.034</b>	<b>-0.807±0.037</b>	<b>-0.801±0.018</b>
	2023-11-17	02:31	60265.605	3120	<b>-0.394±0.024</b>	<b>-0.887±0.020</b>	<b>-0.821±0.029</b>
WD 0549–261	2023-11-18	01:57	60266.581	4800	-0.008±0.086	<b>-0.191±0.050</b>	0.008±0.055
WD 0638–044	2023-03-27	21:42	60031.404	4400	0.286±0.203	0.066±0.101	-0.002±0.095
<b>WD 0654+059 *</b>	2023-03-24	23:18	60028.471	4400	-0.143±0.148	<b>-0.463±0.089</b>	-0.103±0.077
	2023-03-25	22:12	60029.425	5200	<b>-0.279±0.093</b>	<b>-0.466±0.094</b>	-0.219±0.078
	2023-11-18	03:34	60266.649	4160	<b>-0.373±0.050</b>	<b>-0.491±0.055</b>	<b>-0.275±0.064</b>
WD 0714+458	2024-02-04	21:10	60345.382	1680	0.022±0.031	0.060±0.038	0.039±0.034
WD 0726+536	2023-11-19	04:09	60267.6730	5200	0.070±0.136	0.048±0.114	0.095±0.073
<b>WD 0745+115 *</b>	2023-03-23	23:10	60027.465	3120	<b>-1.089±0.053</b>	<b>1.751±0.071</b>	<b>0.874±0.065</b>
	2023-03-25	23:37	60029.484	3120	<b>-1.145±0.067</b>	<b>1.680±0.064</b>	<b>0.878±0.056</b>
	2023-11-17	03:48	60265.658	4080	<b>-1.124±0.063</b>	<b>1.881±0.058</b>	<b>0.906±0.052</b>
	2024-02-04	22:18	60345.429	4800	<b>-1.165±0.046</b>	<b>1.768±0.037</b>	<b>0.895±0.043</b>

Table 2. continued.

STAR	DATE yyyy-mm-dd	UT hh:mm	JD – 2400000	Exp. (s)	V/I (%)		
					B'	V'	R'
WD 0748+614	2023-03-26	23:03	60030.461	2880	-0.007±0.062	-0.008±0.062	-0.018±0.040
WD 0749+426	2022-11-22	03:08	59905.631	5200	0.010±0.117	0.153±0.079	-0.033±0.054
WD 0751+578	2022-11-20	05:50	59903.743	1600	-0.004±0.030	-0.057±0.029	0.023±0.033
<b>WD 0756+437</b>	2022-11-22	01:27	59905.561	3200	<b>6.927±0.041</b>	<b>8.558±0.064</b>	<b>4.702±0.041</b>
	2022-11-22	04:31	59905.688	3200	<b>4.458±0.029</b>	<b>5.539±0.052</b>	<b>3.798±0.044</b>
	2024-02-03	21:59	60344.416	3680	<b>5.041±0.117</b>	<b>5.838±0.159</b>	<b>4.452±0.159</b>
	2024-02-05	22:26	60346.435	3520	<b>6.464±0.070</b>	<b>8.187±0.092</b>	<b>4.698±0.051</b>
	2024-02-06	23:24	60347.475	2880	<b>5.108±0.034</b>	<b>6.332±0.035</b>	<b>4.406±0.040</b>
WD 0759–283	2023-11-18	05:19	60266.721	4800	-0.018±0.047	0.206±0.081	<b>0.193±0.044</b>
WD 0810+489	2022-11-19	05:03	59902.711	1920	-0.041±0.018	0.001±0.023	-0.042±0.028
WD 0847–017	2024-02-05	05:46	60345.504	5600	0.169±0.070	-0.060±0.070	-0.054±0.048
WD 0848+166	2023-03-27	23:07	60031.463	4160	-0.029±0.075	-0.078±0.047	-0.091±0.049
WD 0853–083	2024-02-05	02:04	60345.586	6400	0.051±0.096	-0.166±0.101	0.172±0.062
WD 0900+734	2022-11-21	04:34	59904.690	4160	0.011±0.065	-0.073±0.056	-0.050±0.055
WD 0945+206	2024-02-06	00:22	60346.515	6720	-0.004±0.095	-0.042±0.096	-0.182±0.063
WD 0947+153	2023-03-24	02:04	60027.586	5000	-0.058±0.103	-0.150±0.090	0.066±0.086
WD 0958+206	2024-02-06	02:37	60346.609	6240	-0.093±0.092	-0.041±0.084	0.168±0.057
<b>WD 1008+290</b>	2023-03-26	01:58	60029.582	3960	<b>-8.421±0.107</b>	<b>-7.037±0.109</b>	<b>7.236±0.046</b>
	2023-03-28	01:06	60031.546	4320	<b>-8.585±0.112</b>	<b>-7.132±0.108</b>	<b>7.308±0.044</b>
	2024-02-05	04:13	60345.676	4800	<b>-8.038±0.130</b>	<b>-7.242±0.114</b>	<b>7.185±0.037</b>
	2024-02-08	05:15	60348.719	5120	<b>-8.367±0.118</b>	<b>-7.598±0.119</b>	<b>7.151±0.041</b>
WD 1012+083	2022-11-22	05:51	59905.744	4800	0.120±0.114	0.040±0.081	-0.153±0.056
<b>WD 1036–204</b>	2022-11-21	05:42	59904.738	2640	<b>-4.450±0.060</b>	<b>-6.523±0.037</b>	<b>-9.196±0.032</b>
	2023-11-17	05:18	60265.721	4560	<b>-4.346±0.060</b>	<b>-6.441±0.055</b>	<b>-9.056±0.052</b>
	2024-02-08	03:45	60348.656	3120	<b>-4.598±0.047</b>	<b>-6.254±0.049</b>	<b>-9.219±0.047</b>
WD 1037+103	2023-03-27	01:24	60030.559	4480	0.075±0.067	0.074±0.067	0.021±0.044
WD 1049+411	2023-03-25	02:42	60028.613	3520	-0.018±0.032	-0.014±0.061	0.127±0.043
WD 1055–072	2022-11-19	05:45	59902.740	1920	0.022±0.021	0.017±0.023	0.023±0.023
WD 1122+214	2023-03-24	03:31	60027.647	3960	0.117±0.073	-0.200±0.068	0.031±0.088
WD 1143+633	2023-11-19	04:09	60267.673	1680	0.070±0.136	-0.068±0.046	0.032±0.027
WD 1153+135	2023-03-25	04:06	60028.671	4800	0.263±0.131	0.223±0.097	0.083±0.085
WD 1155+003	2024-02-07	01:05	60347.545	7200	-0.297±0.103	0.099±0.122	0.031±0.062
WD 1223+188	2023-03-27	02:34	60030.607	2640	0.016±0.049	0.009±0.050	-0.061±0.056
WD 1239–133	2024-02-05	06:24	60345.767	3120	0.052±0.029	-0.018±0.034	-0.037±0.032
WD 1245–102	2024-02-06	04:41	60346.695	4160	0.048±0.064	-0.053±0.056	0.037±0.056
WD 1310+027	2022-07-03	22:41	59764.445	6000	-0.300±0.133	-0.312±0.127	0.081±0.084
<b>WD 1315+222</b>	2023-03-26	03:17	60029.637	3600	<b>0.308±0.054</b>	<b>0.224±0.078</b>	<b>0.178±0.047</b>
WD 1343+422	2023-03-26	05:28	60029.728	4320	-0.045±0.100	-0.013±0.090	0.009±0.060
<b>WD 1346+121</b>	2023-03-27	04:10	60030.674	7100	<b>-0.415±0.137</b>	<b>-0.415±0.137</b>	<b>-1.187±0.070</b>
WD 1419+426	2024-02-07	03:03	60347.627	4800	-0.179±0.048	0.095±0.055	-0.022±0.080
WD 1434+437	2024-02-06	06:13	60346.759	4160	0.150±0.069	-0.007±0.062	-0.042±0.050
WD 1533+469	2024-02-07	04:57	60347.706	6240	0.180±0.109	0.174±0.115	0.169±0.080
WD 1547+572	2023-03-28	02:38	60031.610	4800	0.034±0.078	-0.195±0.076	-0.096±0.077
WD 1554–079	2022-07-04	00:42	59764.529	6240	<b>-0.412±0.116</b>	0.019±0.108	0.009±0.086
<b>WD 1556+044</b>	2022-06-28	23:39	59759.485	2880	<b>-0.262±0.038</b>	<b>0.370±0.036</b>	<b>-0.160±0.042</b>
	2022-07-01	23:41	59762.487	3120	<b>-0.264±0.040</b>	<b>0.401±0.038</b>	<b>-0.167±0.042</b>
	2023-03-26	04:17	60029.678	2400	<b>-0.294±0.044</b>	<b>0.261±0.042</b>	-0.119±0.057
WD 1717+104	2023-03-24	05:19	60027.721	6720	0.001±0.139	0.132±0.089	-0.011±0.086
WD 1731+290	2023-03-25	05:35	60028.733	3840	<b>-0.203±0.067</b>	-0.074±0.068	-0.027±0.060
WD 1741+145	2024-02-07	06:22	60347.765	2240	-0.037±0.026	-0.061±0.025	-0.030±0.027

**Table 2.** continued.

STAR	DATE yyyy-mm-dd	UT hh:mm	JD – 2400000	Exp. (s)	$V/I$ (%)		
					$B'$	$V'$	$R'$
WD 1745+290	2023-03-28	04:56	60031.706	5200	$0.077\pm 0.072$	$0.202\pm 0.097$	$0.153\pm 0.064$
<b>WD 1900+705</b>	2023-11-16	20:00	60265.333	600	<b><math>3.709\pm 0.009</math></b>	<b><math>3.499\pm 0.016</math></b>	<b><math>3.784\pm 0.016</math></b>
<b>WD 2049–222</b>	2022-07-03	03:21	59763.639	1680	<b><math>0.093\pm 0.024</math></b>	<b><math>0.122\pm 0.023</math></b>	$0.089\pm 0.039$
<b>WD 2049–253</b>	2022-07-01	03:03	59761.627	2640	<b><math>0.358\pm 0.056</math></b>	<b><math>0.548\pm 0.056</math></b>	<b><math>0.584\pm 0.035</math></b>
	2022-07-04	02:58	59764.624	3120	<b><math>0.354\pm 0.044</math></b>	<b><math>0.551\pm 0.045</math></b>	<b><math>0.656\pm 0.023</math></b>
<b>WD 2211+372</b>	2022-11-18	22:49	59902.451	4160	<b><math>1.192\pm 0.067</math></b>	<b><math>0.538\pm 0.071</math></b>	<b><math>0.407\pm 0.050</math></b>
	2023-11-16	20:57	60265.373	3960	<b><math>1.299\pm 0.060</math></b>	<b><math>0.646\pm 0.063</math></b>	<b><math>0.370\pm 0.058</math></b>
WD 2228+226	2022-07-05	02:27	59765.602	3600	$-0.033\pm 0.067$	$-0.056\pm 0.046$	$0.064\pm 0.045$
	2022-11-19	21:34	59903.399	5200	$-0.046\pm 0.060$	$-0.093\pm 0.082$	$-0.035\pm 0.076$
WD 2303+391	2022-11-20	21:54	59904.412	6240	$-0.054\pm 0.076$	$-0.229\pm 0.105$	$-0.044\pm 0.074$
WD 2345+027	2022-11-19	23:06	59903.463	3960	$0.082\pm 0.077$	$-0.022\pm 0.082$	$0.142\pm 0.090$
WD 2359+636	2022-11-20	00:37	59903.526	4800	$-0.110\pm 0.086$	$-0.120\pm 0.075$	$-0.152\pm 0.063$